SECTION 8.0

... Radio Astronomy Observatory
Post Office Box 2
Green Bank, West Virginia 24944
Telephone Arbovale 456-2011

REPORT NO. H79-7
CONTRACT NO. RAP-79
PAGE ___ OF ___
DATE Mar. 1969

PROJECT: 300 FT. DIA. HOMOLOGY TELESCOPE

SUBJECT: POSITION REFERENCE PLATFORM APPENDIX IV

APPENDIX IV

8.0 GYRO COMPASS - SURVEY

PREPARED BY N. Eklund APPROVED BY ___ SUBMITTED BY S.D.L.

SURVEY OF AZIMUTH-INDICATING INSTRUMENTS FOR RADIO TELESCOPES

8.1 Introduction

The present report describes the findings of the first phase of a study to determine the feasibility of employing a meridian-seeking gyroscope on the moving structure of a large, tracking radio-telescope for the purpose of continuously providing the true azimuth position of the telescope.

In this connection, several U. S. companies, known to be or to have been, active in the field of high accuracy meridian-seeking gyroscopes were contacted, requesting them to indicate whether they could furnish a meridian-seeking gyro that would be expected to achieve the required performance, as outlined in preliminary specifications.

Only two positive reponses to those inquiries were received, namely, from TRW, Redondo Beach, California, and from LSI, Santa Monica, California, both of which firms have considerable experience in this field.

8.2 Preliminary Specifications

The following specifications for the azimuth indicators, located on a horizontally stabilized platform at the apex of the antenna dish, have been supplied to interested parties, and have also been the basis for this report:

1. Tracking accuracy of azimuth indication: ±5 arc.sec. RMS
2. Tracking speed range: $\frac{1}{10} V_s \leq V_t \leq V_s$ (V_s = SIDEREAL VELOCITY)
3. Maximum drive speed at scanning: 5 degrees/min.
4. Linear acceleration of platform due to drive speed: 0.003 cm/sec^2
5. Maximum drive acceleration: 0.5 arcmin/sec^2
6. Linear acceleration of platform due to drive acceleration: 2.03 cm/sec^2

PROJECT: 300 FT. DIA. HOMOLOGY TELESCOPE

SUBJECT: POSITION REFERENCE PLATFORM APPENDIX IV

7. Linear acceleration of platform due to bumps in the azimuth rails: 0.013 cm/sec^2

8. Linear accelerations of platform due to wind gusts on structure:

	Acceleration	Duration of Gust
(a)	0.24 cm/sec^2 $\approx$ 2.4 x 10^{-4}g	$\approx$ 0.1 sec.
(b)	0.13 cm/sec^2 $\approx$ 1.3 x 10^{-4}g	$\approx$ 0.25 sec.
(c)	0.082 cm/sec^2 $\approx$ 8 x 10^{-5}g	$\approx$ 0.5 sec.
(d)	0.051 cm/sec^2 $\approx$ 5 x 10^{-5}g	$\approx$ 1.0 sec.
(e)	0.028 cm/sec^2 $\approx$ 2.8 x 10^{-5}g	$\approx$ 2.5 sec.

9. Vertical acceleration of platform: 0.01 cm/sec^2

10. Levelness of platform: ± 2 arc-sec

11. Environmental temperature of platform: 120°F ±1°F.

12. Readout time after scanning motion has ceased: $\approx$ 1 min.

13. Platform is assumed to be located at the apex of the antenna dish, which is approximately 46 ft. from the intersection of elevation and azimuth axes.

Remarks: In item 6, acceleration is based on the platform being 46 feet vertically above the elevation axis. In item 8, all accelerations are based on the antenna axis being horizontal with the wind face-on.

8.3 Platform Velocities During Tracking Operation

Since the question has been raised as to the effect of the earth's motion on the platform and on the performance of the gyro azimuth indicator, it seems appropriate to determine the angular motion of the platform about its vertical axis during tracking.

Let (X,Y,Z) be a system of coordinates, with its origin at the center of the earth, and rotating with it. Furthermore, let the X-axis point to north, the Y-axis to east, and the Z-axis to the zenith.

NATIONAL RADIO ASTRONOMY OBSERVATORY
POST OFFICE BOX 2
GREEN BANK, WEST VIRGINIA 24944
TELEPHONE ARBOVALE 456-2011

REPORT NO. H79-7
CONTRACT NO. RAP-79
PAGE 8.3 OF
DATE Mar. 1969

PROJECT: 300 FT. DIA. HOMOLOGY TELESCOPE

SUBJECT: POSITION REFERENCE PLATFORM APPENDIX IV

The apparent motion of the star, S, as viewed against the celestial sphere, will be a circle about the earth's polar axis, as shown in the figure below.

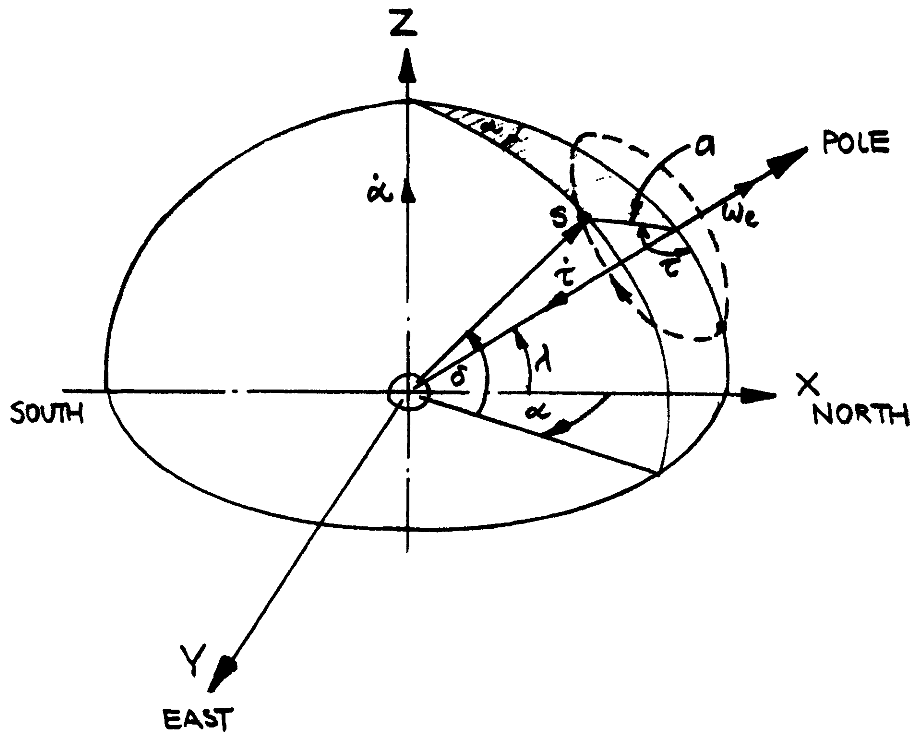

The instantaneous position of the star, S, is given by the coning angle, a, and the hour angle, τ , measured from the point of lower culmination of the star. α and δ are the azimuth and altitude angles, respectively, of the antenna location, relative to both the earth and to the celestial sphere.

From the spherical triangle, outlined in the figure, we have:

$$\cot a \sin(90-\lambda) = \sin(180-\tau)\cot\alpha + \cos(180-\tau)\cos(90-\lambda) \qquad (1)$$

or, after some simplication:

$$\cot a \cos\lambda = \sin\tau\cot\alpha - \cos\tau\sin\lambda \qquad (2)$$

PREPARED BY N. Eklund APPROVED BY SUBMITTED BY S.D.L.

PROJECT: 300 FT. DIA. HOMOLOGY TELESCOPE

SUBJECT: POSITION REFERENCE PLATFORM APPENDIX IV

We wish to obtain the azimuth velocity, $\dot{\alpha}$. Differentiating (2) with respect to time, we have

$$\dot{\alpha} = \frac{[\cos\tau \cot\alpha + \sin\lambda \sin\tau]\,\dot{\tau}}{[1+\cot^2\alpha]\sin\tau} \tag{3}$$

Solving equ. (2) for cotan α , we obtain

$$\cot\alpha = \frac{\sin\lambda\cos\tau + \cos\lambda\cot a}{\sin\tau}$$

and, upon substitution of this expression in equ. (3) we obtain explicitly

$$\dot{\alpha} = \frac{[\sin\lambda + \cos\lambda \cot a \cos\tau]\,\dot{\tau}}{\sin^2\tau + [\sin\lambda\cos\tau + \cos\lambda\cot a]^2} \tag{4}$$

Similarly, for the altitude angle, δ, we have

$$\cos(90-\delta) = \cos(90-\lambda)\cos a + \sin(90-\lambda)\sin a\cos(180-\tau) \tag{5}$$

and after simplification:

$$\sin\delta = \sin\lambda\cos a - \cos\lambda\sin a\cos\tau \tag{6}$$

Differentiating (6) with respect to time, we obtain

$$\dot{\delta} = \frac{[\cos\lambda\sin a\sin\tau]\,\dot{\tau}}{\sqrt{1-[\sin\lambda\cos a - \cos\lambda\sin a\cos\tau]^2}} \tag{7}$$

$\dot{\delta}$ can be resolved into two components:

The north component $\dot{\delta}_N = \dot{\delta}\sin\alpha$

The east component $\dot{\delta}_E = \dot{\delta}\cos\alpha$

Multiplying $\dot{\delta}$ by sin α and cos α , respectively, gives then

$$\dot{\delta}_N = \frac{[\cos\lambda\sin a\sin^2\tau]\,\dot{\tau}}{\left\{[1-(\sin\lambda\cos a - \cos\lambda\sin a\cos\tau)^2][\sin^2\tau + (\cos\lambda\cot a + \sin\lambda\cos\tau)^2]\right\}^{\frac{1}{2}}} \tag{8}$$

$$\dot{\delta}_E = \frac{[\cos^2\lambda\cos a + \cos\lambda\sin\lambda\sin a\cos\tau]\,\dot{\tau}}{\left\{[1-(\sin\lambda\cos a - \cos\lambda\sin a\cos\tau)^2][\sin^2\tau + (\cos\lambda\cot a + \sin\lambda\cos\tau)^2]\right\}^{\frac{1}{2}}} \tag{9}$$

PREPARED BY N. Eklund APPROVED BY SUBMITTED BY S.D.L.

PROJECT: 300 FT. DIA. HOMOLOGY TELESCOPE

SUBJECT: POSITION REFERENCE PLATFORM APPENDIX IV

Relative to inertial space, the angular velocity of the point of observation is $\dot{\tau}\sin\lambda$ about the vertical axis and $\dot{\tau}\cos\lambda$ about the north-axis.

The motion of the platform relative to inertial space is then given by the resultant velocities about the three axes. Thus, with $\dot{\tau} = -\omega_e$, we obtain the following inertial velocity components:

$$\begin{cases} \dot{\alpha}_i = \omega_e \sin\lambda + \dot{\alpha} \equiv \omega_e\left[\sin\lambda - \varphi(\lambda, a, \tau)\right] \\ \dot{\delta}_{Ni} = \omega_e \cos\lambda + \dot{\delta}_N \equiv \omega_e\left[\cos\lambda - \psi(\lambda, a, \tau)\right] \\ \dot{\delta}_{Ei} = \dot{\delta}_E \equiv \omega_e \xi(\lambda, a, \tau) \end{cases} \tag{10}$$

Now, if the platform is mounted on the antenna, and if it is slaved to the local gravity vector, then the relative velocities with respect to earth, $\dot{\delta}_N$ and $\dot{\delta}_E$, will vanish. Under these conditions, the absolute velocities experienced by the platform will be reduced to:

$$\begin{cases} \dot{\alpha}_i = \omega_e\left[\sin\lambda - \varphi(\lambda, a, \tau)\right] \\ \dot{\delta}_{Ni} = \omega_e \cos\lambda \\ \dot{\delta}_{Ei} = 0 \end{cases} \tag{11}$$

It is seen from equ's (11) that the north and the east components of the platform motion are identical to those of a stationary gyro support at that latitude. The vertical component, on the other hand, has a supplementary velocity, $\omega_e \varphi(\lambda, a, \tau)$, which varies both in magnitude and direction. Furthermore, if the apparent orbit of the star passes close to the zenith, then the supplementary velocity becomes very large in comparison with the stationary vertical velocity, $\omega_e \sin\lambda$, and grows beyond bounds, if the orbit passes through the zenith.

In principle, the behavior of a meridian seeking gyro would be entirely unpredictable under these conditions, since the function $\varphi(\lambda, a, \tau)$, and its first four time derivatives, will enter into the equations of motion of the gyro. Since in addition hereto, the coning angle, a, varies virtually from star to star, it would be an impossible task to interpret the gyro motion.

PREPARED BY N. Eklund APPROVED BY SUBMITTED BY S.D.L.

Fortunately, however, the effect of the supplementary vertical velocity, $\omega_e \varphi(\lambda, a, \tau)$, can be removed in a very simple way, namely, by slaving the gyro support to the meridian, and letting the instrument housing rotate with the platform.

Consequently, with the gyro spin axle resting in the meridian plane, the follow-up motor will drive the gyro support, so as to zero the pickoff between the gyro and the support, and thus maintain the support in alignment with the gyro. Under these conditions, the gyro will only experience the vertical velocity $\omega_e \sin \lambda$, and the horizontal velocity $\omega_e \cos \lambda$, which are the same velocities, as it would experience if it were stationary on the ground.

8.4 Range of the Supplementary Vertical Velocity

Although the supplementary velocity is cancelled out relative to the gyro, bounds must be set for the maximum velocity and acceleration that can be tolerated about the vertical axis.

The maximum value of $\varphi(\lambda, a, \tau)$, for constant values of λ and a, occurs when the star passes through its upper culmination point. At this point the distance to the zenith is the co-altitude:

$$\varepsilon_z = \frac{\pi}{2} - \delta_z$$
$$= \frac{\pi}{2} - \lambda - a$$

The supplemental velocity, $\dot{\alpha} = \omega_e \varphi(\lambda, a, \tau)$, and the acceleration, $\ddot{\alpha} = \omega_e^2 \frac{d\varphi}{d\tau}$, about the vertical axis, are of interest in determining the performance of the meridian seeking gyro. From equ. (4) we calculate the ratio $\dot{\alpha}/\omega_e = \varphi(\lambda, a, \tau)$, and then obtain the ratio $\ddot{\alpha}/\omega_e^2$ by differentiation. We are only interested in maximum values of the azimuth velocity, as the star passes through the upper culmination point, Likewise, we wish to know the maximum acceleration, which we approximate from the maximum value of the tangent to the azimuth velocity curve. The calculated data are given below for the co-altitude angles ε_z = 2°, 3°, 4°, 5° and for λ = 38°:

$\varepsilon_z{}^\circ$	$\dot{\alpha}/\omega_e$	$\dot{\alpha}$ RAD/SEC	$\ddot{\alpha}/\omega_e^2$	$\ddot{\alpha}$ RAD/SEC^2
2	24	1.75×10^{-3}	380	2×10^{-6}
3	15.5	1.13×10^{-3}	150	$.8 \times 10^{-6}$
4	11.2	$.82 \times 10^{-3}$	110	$.58 \times 10^{-6}$
5	8.38	$.61 \times 10^{-3}$	70	$.37 \times 10^{-6}$

The maximum values of $\dot{\alpha}$ and $\hat{\dot{\alpha}}$ are seen to be quite low, and will not have any detrimental effect on the performance of the meridian seeking gyro.

8.5 Types of Meridian Seeking Gyros

Currently available meridian seeking gyros can be divided into two distinct types:

(a) Rate Integrating Gyros
(b) Pendulous Gyros

8.5.1 The Rate Integrating Gyro

This gyro represents the simplest approach to a meridian seeking instrument. A single-degree-of-freedom gyro is mounted with its spin axle horizontal and its frame rotatable about a vertical axis. The directive moment of the gyro is proportional to the horizontal component, $\omega_e \cos\lambda$, of the earth's velocity, and to the deviation, ψ, of the spin axis from the meridian: $M_D = H\omega_e \cos\lambda \sin\psi$. Consequently, if there are no spurious torques about the input axis, and if the output axis is truly vertical, then there will be no torques acting on the gyro, when it is resting in the meridian plane. By equipping the gyro output axis with an electromagnetic pickoff and a torquer in a high-gain feedback loop, it is possible to achieve a very high rate sensitivity, as well as very high null stability.

While the rate integrating gyro can be made to indicate the meridian with a 1σ error of only a few arcseconds, this can only be achieved under the most ideal conditions, such as when the instrument is mounted on a solid, rigid and vibration-free foundation. Also, this accuracy is based on taking four readings, including rotating the spin axle through 180°, and then taking the average of the four readings. This procedure requires between 30 and 40 minutes for one determination of the meridian. Gyros of this type have been developed and built by Autonetics and TRW.

From the known characteristic features of the rate integrating gyro with its sensitivity to spurious rates, it is concluded that <u>this type of gyro will be both impractical and unsatisfactory</u> for the application in question.

8.5.2 The Pendulous Gyro

8.5.2.1 Principle of Pendulous Meridian-Seeking Gyros

The pendulous gyro is characterized by having two degrees of freedom, and by having its center of gravity below its center of support. It can, thus be considered as being a spherical pendulum.

The pendulous meridian-seeking gyro is suspended with its spin axle horizontal and with the rotor spinning in the same direction as the earth.

If the spin axis of the gyro is to stay in the meridian plane, then the gyro spin axle must precess about the vertical with the same velocity as the meridian plane rotates relative to inertial space, i.e., it must have the constant precessional velocity $\omega_e \sin\lambda$.

To do this, the spin axle of the gyro must be tilted upwards, such that the pendulous moment, created by the tilt, will produce the required precession velocity. If the precession rate of the gyro is higher, or lower, than the correct rate, then the spin axle will tend to lead, or lag, the rotation of the meridian plane. In the first case, the pendulous moment will decrease and the precession rate will slow down, while in the second case, the pendulous moment will increase, and speed up the precession. Consequently, the only equilibrium position of the gyro spin axle is in the meridian plane, and any deviation from this position will generate a precession moment to restore the system to its equilibrium position, relative to the earth.

To enable the gyro to precess at the constant rate required to keep pace with the meridian plane, it must be acted upon by a constant torque about the elevation axis. This torque is produced by a constant upward tilt of the spin axle; as a consequence, the spin axis is not horizontal, when at rest in the meridian plane, but forms a small elevation angle $\theta_0 \approx \frac{H\omega_e \sin\lambda}{M}$ This angle is only a few seconds of arc.

8.5.2.2 Types of Pendulous Gyros

The pendulous gyro has been used in various modifications for the last 60 years, and has achieved great success as a marine compass on board ships. There are, at least, five basic variations of this type of gyro, based on the particular mode of suspension:

(1) Conventional two-gimbal gyro
(2) Band or wire suspended gyro
(3) Liquid-floated gyro
(4) Universal support, pressurized air-bearing gyro
(5) Universal support, gas-squeeze bearing gyro

In addition, there are many hybrid suspensions, such as a two-gimbal system with wire suspension to reduce the load on the azimuth bearings, band suspension systems with a buoyancy liquid to reduce the load on the band, as well as many others.

Furthermore, any one of the above types may be damped, so as to come to rest in the meridional plane in a relatively short time (one-half to two periods of the characteristic oscillation), or it may be, virtually, undamped and perform an angular oscillation about the meridional plane, the latter being the bisector of the total angle of the oscillation.

In the present application, in which continuous recording of the azimuth position is desired, only the damped type is of interest; an undamped, oscillatory gyro would require a computer to determine the average azimuth angle from the gyro oscillations which are superimposed on the actual azimuth motion of the antenna. A further advantage of the damped gyro is thatif a momentary disturbance tends to drive the gyro away from the meridional plane, the damping torque will oppose this motion and thus reduce the deviation of the gyro from the meridional plane.

8.5.2.2.1 The Two-Gimbal Gyro

In this instrument, the pitch and yaw gimbal axes are perpendicular to each other and to the gyro spin axle, when the latter is horizontal. The center of gravity of the gyro casing lies below the intersection of the gimbal axes, thus making the gyro pendulous. However, this type of gyro does not offer very high accuracy, due to the unavoidable friction in the gimbal bearings. In spite of this, it has been very successful as a marine compass.

The reason for this is twofold: First, the accuracy required of a marine compass is not very high; 5-15 arcmin. is, probably, the requirement for a high-quality marine compass. Secondly, in order to minimize the effect of the gimbal bearing friction, gyro rotors of enormous angular momentum are employed, the largest marine compass having a gyro angular momentum equal to about 1,000 times that used in a high-accuracy, stationary, meridian-seeking gyro.

In recent years, the gimbal bearing friction has been considerably reduced by impressing an oscillatory motion on the gimbal bearing races. However, this type of suspension is definitely ruled out for the present application.

8.5.2.2.2 <u>The Band-Suspended Gyro</u>

This type of suspension has been employed extensively in meridian-seeking gyros for stationary applications. The gyro proper is generally mounted in a vertically suspended cylinder. The suspension means is generally a band, rather than a wire, since one strives to make the torsion moment of the suspension as low as possible for a given stress. For the same reason, the suspension band is made as long as possible, consistent with the height of the instrument housing.

The band suspension offers a number of advantages over the gimbal-mounted gyro. First, there is, of course, no gimbal bearing friction, but the gyro is completely free from constraints about the vertical (output) axis. This is achieved by using a servo follow-up, whereby the upper band clamp is made to track the lower band clamp with a lag of only a few arcsec. Since the lower band clamp is rigidly mounted on the gyro container and thus has a fixed orientation to the gyro spin axle, while the upper band clamp is rigidly connected to the output shaft, One sees that the motion of the output shaft is virtually a replica of the azimuth motion of the gyro and can, therefore, be used to drive a Theodolite or an encoder for readout of the azimuth position of the gyro.

Secondly, the band suspension acts as a filter against external disturbances, in the same way as a conventional pendulum. But, as a pendulum, it also has resonant frequencies, which must be considered against the background of disturbances, to which the instrument will be exposed. Damping means, using liquid, air or eddy currents, are generally provided to minimize the sensitivity to resonant excitation.

Thirdly, the band-suspended gyro is, essentially, unaffected by minor dislevelments of its base, or platform. Generally, dislevelments up to one arcmin. have little or no effect on the accuracy of the gyro.

The accuracy of the band-suspended gyro is definitively in the range of the accuracy of the present application. This type of meridian-seeking gyro has been developed, primarily, by L.S.I.

8.5.2.2.3 The Liquid-Floated Gyro

This type of gyro suspension is probably the first practical method of frictionless support for a gyro, having been proposed as early as 1884 by Lord Kelvin who, incidentally, also experimented with a torsion-free band-suspension. However, it was not until 1908, when Anschütz-Kampfe, together with Max Schuler developed and patented his mercury-floated gyro, that a serviceable gyro compass became a reality. Since then, this type of gyro compass has been greatly improved, especially through the efforts of Schuler, so that it is now looked upon as a monument to engineering science.

As in the case of the band-suspended gyro, the liquid floated gyro has no gimbal bearing friction to contend with. The gyro proper is either mounted inside the float, as in the Anschütz compass, or it may be mounted below the float, in a frame supported by the buoyancy of the float. A precision servo constrains the fluid container to track the azimuth motion of the gyro with but a few arcsec. lag.

In the floated gyro instruments built today, mercury is no longer used as the buoyant liquid, but has been replaced by a viscous fluorocarbon liquid. This does not interfere with the motion of the gyro float, since both the liquid and the liquid container rotate with the float. Furthermore, the azimuth precession of the gyro is so slow that, even without the follow-up, the gyro would not be measurably affected by the viscous drag. However, in the case of lateral disturbances that tend to excite some of the pendulous modes of oscillation, the fluid acts to prevent the buildup of resonant motion.

In general, with one exception, it can be said that the liquid supported gyro has the same advantages as the band-suspended gyro over the gimbal supported gyro. The one exception is the need for heating of the liquid at low temperatures, and the concomitant disturbing effects of convection currents. However, this should not be of any consequence in the present application.

The accuracy of this type of gyro is decidedly in the range of the accuracy desired in the present application.

8.5.2.2.4 Pressurized Air-Bearing Supported Gyro

This gyro employs a concave spherical base, upon which the convex spherically shaped gyro case is supported by a layer of compressed air. The air is fed in under pressure through a number of capillaries in the base surface, and escapes radially at the circumference of the base.

This method of support has been widely used in all types of bearings to create a frictionless state. It has been quite successful in many applications, including gyros, but has not been satisfactory as universal support for a meridian-seeking gyro.

The reason for this failure is due to the fact that the air, escaping at the rim of the bearing, has not a purely radial motion, but has also some tangential components, due to the lack of perfection of the matching surfaces. As a consequence, so-called "turbine torques" are generated at the rim of the supported bearing surface, which tend to drive the gyro off the meridian in one direction or the other, depending on the momentary state of the flow.

It does not seem likely that this type of support can guarantee a better accuracy than, say, one arcmin. Consequently, this gyro cannot be considered for the present application.

8.5.2.2.5 Universal Gas Squeeze-Bearing Gyro

As in the case of the externally pressurized air bearing gyro, the gas squeeze-bearing consists of a concave, spherical base and a convex, spherically shaped, gyro case supported on a film of compressed air. The difference between the two methods of support lies in the way the air cushion is generated and in the pattern and the magnitude of the air flow between the bearing surfaces.

In the gas squeeze-bearing, the pressurized gas film between the two bearing surfaces is generated by oscillating the supporting bearing surface in the vertical direction at an ultrasonic frequency of, say, 20,000 Hz or higher, by means of a piezoelectric or magnetostrictive transducer.

Phenomenologically, the gas squeeze-bearing effect can be explained in terms of Boyle's Law for the isothermal state of gas: PV = const. For this purpose, consider two flat, parallel, opposing discs with rather small clearance, one stationary while the other one is oscillated normal to its surface. At sufficiently high frequencies of oscillation, the viscous forces become effective in opposing the radial flow, and compressibility effects come into play. As a result, the gas flow is limited to a narrow region at the rims, and a small amount of gas is trapped in the clearance between the two discs. Its state can be approximately described by Boyle's Law, applied to this small, periodically variable volume.

It should be noted that Boyle's Law is not a linear one, and this is essentially the fact that accounts for the "squeeze" effect, since the time average of the perturbed pressure over one period of oscillation will exceed the unperturbed pressure (i.e., the environmental pressure); the net difference between the two is the squeeze-bearing effect.

The average clearance between the surfaces of the gas squeeze bearing is only about 10^{-4} inches, i.e., about 1/10 of the clearance of an externally pressurized gas bearing of this type. Consequently, a very small gas volume is trapped between the surfaces, which circumstance, coupled with the short time between reversals, (5×10^{-5} sec.) is responsible for the absence of the turbine torques that mar the performance of the externally pressurized, universal bearing.

The bearing can be driven efficiently by means of a piezoelectric transducer. An experimental gyro, supported in this manner and weighing about 7 lbs., required only a 2" diam. bearing surface, and an electrical input to the transducer of less than one watt. This gyro is an LSI development.

The gas squeeze bearing gyro is, potentially, superior to other types of meridian seeking gyros, but requires further development for a practical application, as in the present case.

8.5.2.3 Operational Features

The three types of meridian seeking gyros that can be considered to be candidates for the present application have, generally, the same operational features:

The gyro motors will be of the synchronous type and equipped with self-activated gas bearings for vibration-free running and long-life operation. They will reach synchronous speed in from 4 to 6 minutes, depending on the size of the gyro.

The gyrowheel of the LSI meridian-seeking gyro, developed for the azimuth laying of the Pershing Missile, has an angular momentum of 35×10^6 gr cm^2/sec. It is damped to the meridian by means of a torquer consisting of two magnet coils at right angles to each other, one secured to the gyro container and the other to the followup. The current in one coil is constant, while the current in the other coil is made proportional to the azimuth velocity of the gyro by means of a velocity generator, mounted on the followup servomotor shaft. The damping is such that the settling motion of the gyro is sub-critical, resulting in a small overshoot of the meridian. However, in the present case, where the spin axle is required to lie continuously in the meridian plane, a somewhat higher, but still sub-critical, damping might be more favorable.

The gyro is designed with a 17 bit encoder, the rotor of which is driven by the followup servo. The present encoder can readily be replaced by an 18 bit encoder, if necessary.

The gyro will reach the meridian from any position within the linear range in about 10 minutes. However, with a timer and high relative damping, the settling time can be reduced to about 1/4 period of the azimuth motion, or to about 80 seconds.

The spacing between the gyro container and the followup cylinder is only about 60 mils, which results in powerful damping of lateral oscillations of the gyro container.

NATIONAL RADIO ASTRONOMY OBSERVATORY
POST OFFICE BOX 2
GREEN BANK, WEST VIRGINIA 24944
TELEPHONE ARBOVALE 456-2011

REPORT NO. H79-7
CONTRACT NO. RAP-79
PAGE 8.15 OF
DATE Mar. 1969

PROJECT: 300 FT. DIA. HOMOLOGY TELESCOPE

SUBJECT: POSITION REFERENCE PLATFORM APPENDIX IV

The figure below is a schematic of the principal elements of the LSI meridian-seeking gyro:

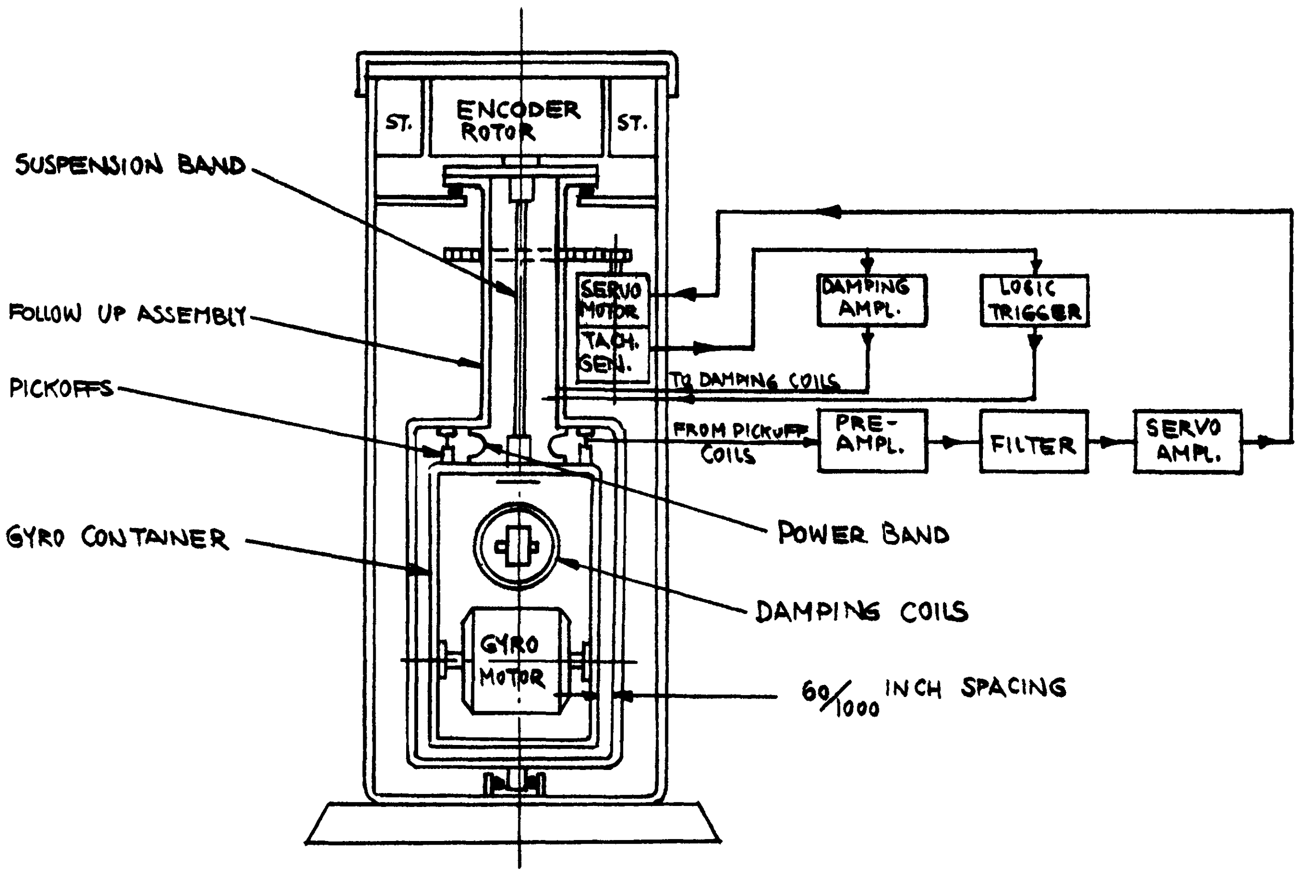

The velocity of the followup motion must have such a range that it can follow the max. azimuth velocity of the antenna. If this be taken to be that occurring at a co-altitude of 2°, and which has been found to be 24 times sidereal speed, or 6°/min., then no difficulties will be encountered as far as the followup motion is concerned.

PREPARED BY N. Eklund APPROVED BY SUBMITTED BY S.D.L.

PROJECT: 300 FT. DIA. HOMOLOGY TELESCOPE

SUBJECT: POSITION REFERENCE PLATFORM APPENDIX IV

The TRW floated, pendulous gyro operates very much in the same fashion as described above in connection with the LSI band-suspended gyro. The pickoffs and the damping arrangement may differ in some details, but the mode of operation and the results are quite similar to those obtained with the LSI instrument. The major difference is in the lateral damping, which is liquid in the TRW instrument, in contrast with the air damping in the LSI instrument. Also, the TRW gyro wheel has an angular momentum of only 10 x 10^6 gr cm^2/sec., but this might very well be sufficient in the absence of parasitic torques. However, if a study should reveal the need for a higher angular momentum, a larger wheel can readily be installed.

The TRW meridian seeking gyro is shown schematically in the diagram below:

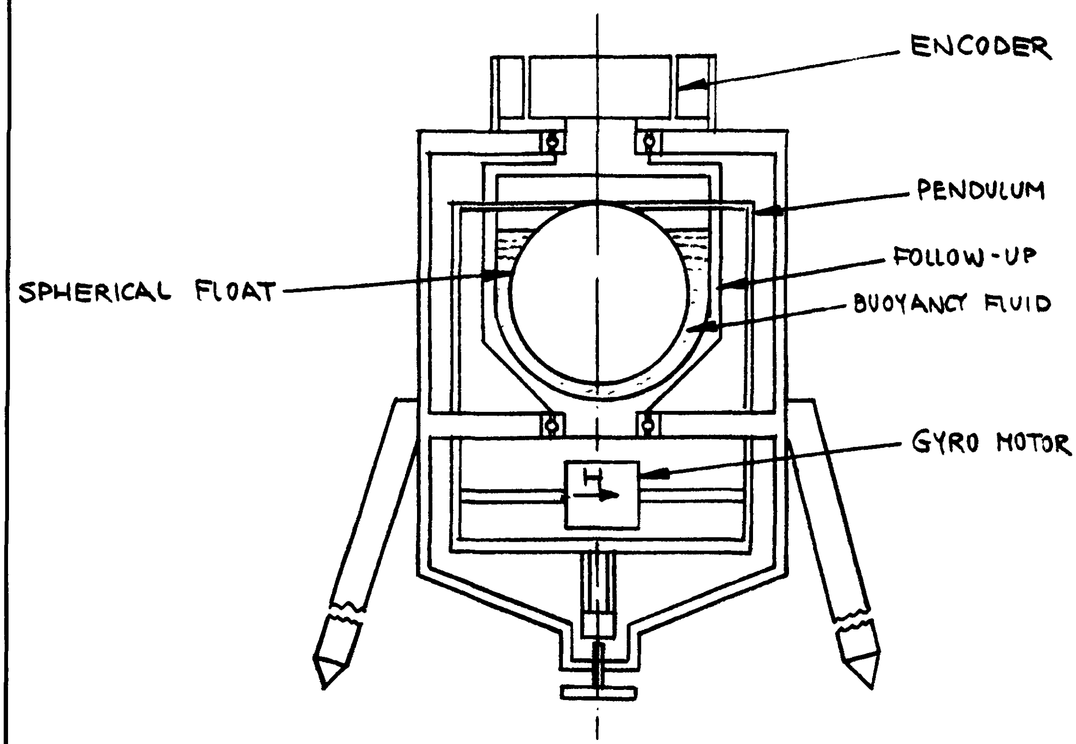

Pickoffs and damping coils are not shown, but will be similar to those in the LSI system.

NATIONAL RADIO ASTRONOMY OBSERVATORY
POST OFFICE BOX 2
GREEN BANK, WEST VIRGINIA 24944
TELEPHONE ARBOVALE 456-2011

PROJECT: 300 FT. DIA. HOMOLOGY TELESCOPE

SUBJECT: POSITION REFERENCE PLATFORM APPENDIX IV

The gas squeeze bearing gyro is shown schematically below:

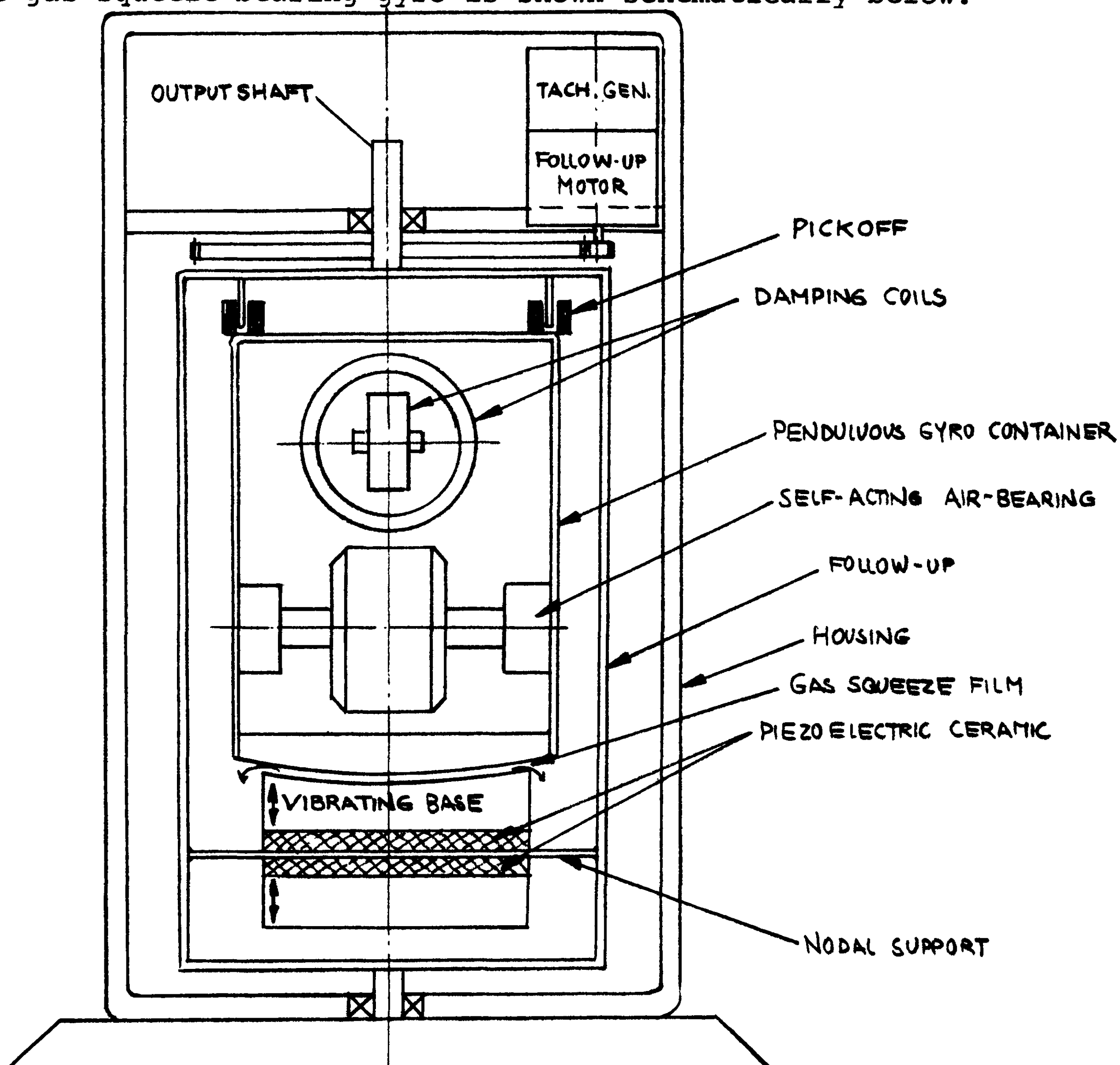

As stated earlier, it is still not fully developed for followup operation, and the schematic arrangement shown is not necessarily an optimum. A better arrangement may be to fix the nodal support to the stationary housing and just rotate the pickoffs, one damping coil and the output shaft.

PREPARED BY N. Eklund APPROVED BY SUBMITTED BY S.D.L.

NATIONAL RADIO ASTRONOMY OBSERVATORY
POST OFFICE BOX 2
GREEN BANK, WEST VIRGINIA 24944
TELEPHONE ARBOVALE 456-2011

PROJECT: 300 FT. DIA. HOMOLOGY TELESCOPE

SUBJECT: POSITION REFERENCE PLATFORM APPENDIX IV

The piezoelectric transducer is driven by a single transistor amplifier. By appropriate positive feedback from the transducer, the latter becomes a self-sustained oscillator, requiring no frequency control to remain in its resonant state.

An interesting aspect of this type of gyro system is that it does not require a large angular momentum, a wheel of 2×10^6 gr cm^2/sec. being sufficient. This is, however, of minor importance in the present application.

8.6 Conclusions

Based on this general investigation, and from the knowledge of the behavior of the various types of meridian seeking gyros, it is concluded that the band-suspended gyro, the floated gyro, and the gas squeeze bearing gyro should all be capable of meeting the requirements of the specifications. All three gyro systems readily admit of modifications to alter their resonant frequencies, so as to minimize the response to certain disturbances.

The major concern is that of torque rectification about the output axis due to periodic disturbances, acting intercardinally on the gyro. However, it is felt that the air damping in the band suspended gyro and the fluid damping in the floated gyro will greatly diminish this threat to the maintenance of the required accuracy.

Another concern is the accelerations due to the bumps in the rails, when the azimuth velocity goes beyond $2\omega_e$. The variation of ±0.5 inches in a 30 ft. length is considered unreasonable; with a track carefully laid on concrete, there should be no difficulty in maintaining the horizontality of the track better than ±0.1 inches in a 10 foot length.

The settling time of one minute, after tracking or slewing motion has ceased, cannot be met. It contradicts the requirement for a low frequency system to obviate effects of noise and periodic disturbances. The shortest settling time would appear to be about 75 seconds after the slewing or scanning operations have ceased.

PREPARED BY N. Eklund APPROVED BY SUBMITTED BY S.D.L.

OPERATED BY ASSOCIATED UNIVERSITIES, INC., UNDER CONTRACT WITH THE NATIONAL SCIENCE FOUNDATION

However, since the gyro spin axle is already in the meridian plane, before slewing or tracking motion begins, it is not expected that the spin axle will deviate from the meridian plane during the ensuing slewing and tracking motions. Consequently, the question of settling time appears to be of no consequence, since the spin axle is constrained to remain in the meridian plane at all times, with the possible exception that the azimuth drive might have been operated, while the gyro was caged. In this case, the gyro spin axle will not be in the meridian plane, when the gyro is uncaged, but will then require 75 seconds to swing into the meridian plane.

8.7 Recommendations

It is not possible to determine, offhand, whether a meridian-seeking gyro will be capable of maintaining the required accuracy under various operating conditions, and for the disturbances outlined in the specifications. This can only be determined from an accurate error analysis of the gyro system, taking into account the simultaneous effect of co-existing disturbances.

It is, therefore, recommended that an error analysis be authorized for the three systems considered above, and that whatever modifications are required for compliance with the specifications be considered and made part of the analysis.

The simplicity of the meridian-seeking gyro system, its immunity to all kinds of weather, and its independence of cooperative, ground-based apparatus and devices should provide the motivation for further study and analysis to determine its practicability for the intended use.